

# PHASE TRANSITIONS IN PLANAR BILAYER MEMBRANES

STEPHEN H. WHITE

*From the Department of Physiology, California College of Medicine,  
University of California, Irvine, California 92664*

**ABSTRACT** Temperature-dependent structural changes in planar bilayer membranes formed from glycerol monooleate (GMO) dispersed in various *n*-alkane solvents (C12-C17) have been studied using precise measurements of specific geometric capacitance ( $C_g$ ).  $C_g$  generally increases as temperature ( $T$ ) decreases. A change in the slope of  $C_g(T)$  occurs between 15 and 18° C for all solvent systems examined. Measurements of the interfacial tension ( $\gamma$ ) of the bulk GMO-alkane dispersions against 0.1 M NaCl show that  $\gamma$  generally decreases with decreasing temperature. The data can be fitted with two straight lines of different slope which intersect on the average at 17° C. Pagano et al. (1973, *Science (Wash. D.C.)*, 181:557) have shown using calorimetry that GMO has a phase transition at about 15° C. Thus, the changes in  $C_g$  and  $\gamma$  with temperature are likely to result from a GMO phase transition. A second structural change is observed to occur between 5 and 10° C which has not been detected calorimetrically. Calculations of  $C_g$  based on various estimates of the hydrocarbon dielectric coefficient ( $\epsilon_B$ ) and/or hydrocarbon thickness ( $\delta_B$ ) lead to models for the structure of the bilayer above and below the phase transition temperature.

## INTRODUCTION

It is generally accepted that the lipids of biological membranes are arranged predominantly in a bilayer configuration. Evidence for this conclusion comes from studies of a variety of membranes using X-ray diffraction (Engelman, 1971; Wilkins et al., 1971), calorimetry (Steim et al., 1969), electron spin resonance (Hubbel and McConnell, 1969), and freeze fracture electron microscopy (Branton, 1966). As the temperature of the lipids is raised above the transition temperature, a gel-to-liquid crystalline phase change occurs which can affect transport processes (Overath et al., 1971) and enzyme activity (Eletr et al., 1973). Phase transitions have been studied extensively in model systems of membrane lipids dispersed in an aqueous phase (e.g., Ladbroke and Chapman, 1969; Melchior and Morowitz, 1972; Hinz and Sturtevant, 1972; Tardieu et al., 1973). Few studies, however, have been made of phase transitions in planar bilayer membranes of the type first described by Mueller et al. (1962). Krasne et al. (1971) examined the effect of phase transitions on ion transport by nonactin and valinomycin in glyceride-decane bilayer films. Carrier-mediated transport was dramatically reduced below the transition temperature ( $\sim 40^\circ$  C). A similar study was per-

formed by Stark et al. (1972) on films formed from homogeneous synthetic lecithins, *n*-decane, and butanol or chloroform. Pagano et al. (1973) measured the optical reflectivity of films formed from glycerol monostearate (GMS) dispersed in *n*-hexadecane above and below the phase transition of the GMS ( $\sim 60^\circ\text{C}$ ). Their data suggested that the thickness of the bilayer increases below the phase transition consistent with X-ray diffraction experiments (Chapman et al., 1967) and theoretical expectations (Träuble, 1972). However, their results may be due in part to the formation of microlenses which can cause high apparent reflectivities.

Measurement of the specific capacitance ( $C_g$ ) of planar bilayer membranes is an excellent method for examining structure since  $C_g$  depends upon the dielectric coefficient and thickness (Hanai et al., 1964; White, 1970*a*; White and Thompson, 1973). These parameters in turn depend upon membrane composition and the molecular properties of the constituents. Thus, measurements of  $C_g$  can provide useful information about temperature-dependent structural changes in planar bilayer membranes (White, 1970*a,b*). High precision determinations of specific capacitance as a function of temperature for bilayer films formed from glycerol monooleate (GMO) and *n*-hexadecane (C16) have been reported by White (1974). Calorimetric studies on bulk aqueous-GMO-C16 systems by Pagano et al. (1973) indicate that the two aliphatic components have phase transitions at about  $15^\circ$  and  $18^\circ\text{C}$ , respectively. White observed the specific capacitance to increase from  $0.625\ \mu\text{F}/\text{cm}^2$  at  $25^\circ\text{C}$  to  $0.745\ \mu\text{F}/\text{cm}^2$  at  $1^\circ\text{C}$ . He suggested that somewhere between the transition temperature for GMO and C16 ( $16^\circ\text{C}$ ) the solvent disproportionates into microlenses and freezes leaving extensive regions (85% or more of area) largely free of solvent. Part of the increase was attributed to an average decrease in membrane thickness caused by this solvent "freeze-out" process. The remainder of the increase is likely due to a phase transition of the GMO.

The purpose of this paper is to report the results of a study of phase transitions in planar bilayer membranes formed from glycerol monooleate (GMO) dispersed in a series of normal alkane solvents. Measurements of specific geometric capacitance ( $C_g$ ) were used to obtain information on the temperature dependence of the thickness and dielectric coefficient of the bilayer. Since  $C_g$  depends upon both thickness and dielectric coefficient, one of these parameters had to be estimated independently to determine the other. Calculations of  $C_g$  resulted in detailed structural models of the planar bilayer membranes.

## METHODS AND MATERIALS

### *Specific Geometric Capacitance*

The specific geometric capacitance of a planar bilayer membrane is given by  $C_g = \epsilon_o \epsilon_B / \delta_B$  where  $\epsilon_o = 8.854 \times 10^{-14}\ \text{F}/\text{cm}$ ,  $\epsilon_B$  is the dielectric coefficient of the hydrocarbon portion of the film, and  $\delta_B$  is the thickness.  $C_g$  for GMO films was calculated from measurements of the apparent specific capacitance ( $C_m$ ) of the bilayer as described by White (1973).  $C_m$  was determined with a precision of  $\pm 0.3\%$  and an accuracy of  $\pm 1\%$  from measurements of total capacitance

( $C_T$ ) and membrane area ( $A_m$ ) using the relation  $C_m = C_T/A_m$  (White, 1970*a*; White, 1973; White and Thompson, 1973). All measurements were made at a frequency of 100 Hz. The AC voltage across the bilayer-electrolyte system was kept constant at 7 mV root mean square.

### Interfacial Tension

The sessile drop method of Staicopolus (1962) was used to determine the interfacial tension of aqueous droplets resting on a Teflon pedestal immersed in the bulk GMO-alkane solution. The pedestal was contained in a standard 1 cm cuvette placed in a brass thermostat through which water from a Lauda K-2/R bath (Brinkmann Instruments, Inc., Westbury, N.Y.) was circulated. Triplicate photographs were made of the droplets at each temperature. The equatorial diameter and height of a droplet were determined in triplicate from each photograph using a Gaertner Scientific Corp. (Chicago, Ill.) microcomparator. The density of the aqueous solutions and the bulk lipid solutions were determined as a function of temperature using the pycnometric method of Lipkin et al. (1944). The acceleration ( $g$ ) due to gravity was calculated from Helmut's equation (*CRC Handbook of Chemistry and Physics*).

### Physical Properties of the Hydrocarbons

The specific geometric capacitance ( $C_g$ ) expected of bilayers in a fluid state (i.e. above the transition temperature) can be calculated using the assumptions of Fettiplace et al. (1971) and the equations of White (1974). Important parameters in these equations are the density of the alkane solvent and the acyl chains of the GMO (taken as equivalent to 1-heptadecene). The densities of these compounds were determined as a function of temperature using the pycnometric method of Lipkin et al. (1944) or from data published by the American Petroleum Institute (1953). The densities ( $\rho$ ) of the compounds are linear functions of temperature ( $T$ ) and the data were fitted to the equation  $\rho = g + hT$  using the method of least squares where  $g$  and  $h$  are constants. The results are shown in Table I. Various other parameters are also required to calculate  $C_g$ . These were obtained from the *CRC Handbook of Chemistry and Physics* and are summarized for convenience in Table II. The dielectric coefficients of the various compounds were calculated from  $\epsilon = n_D^2$  where  $n_D$  is the index of refraction at 20°C at the wavelength of the sodium  $D$  line. Changes in  $\epsilon$  with temperature above the transition were calculated as described by White (1974).

TABLE I  
TEMPERATURE DEPENDENCE OF THE DENSITIES OF VARIOUS ALIPHATIC  
HYDROCARBONS DETERMINED USING THE PYCNOMETRIC METHOD  
OF LIPKIN ET AL. (1944)

The data were fitted to the equation  $\rho(T) = g + hT$ . These data are used to calculate membrane dielectric coefficient and thickness using the equations of White (1974) (see Appendix).

Hydrocarbon	Temperature range	$g \pm \text{SD}$	$h \pm \text{SD}$	Correlation coefficient	Calculated $\rho(20)$
		$\text{g/cm}^3$	$10^{-4} \text{ g/cm}^3/^\circ\text{C}$		
<i>n</i> -dodecane	3.2–30.0	$0.7621 \pm 0.0006$	$-6.810 \pm 0.326$	-0.989	0.7485
<i>n</i> -tetradecane	8.0–30.0	$0.7763 \pm 0.0002$	$-6.801 \pm 0.124$	-0.998	0.7627
<i>n</i> -hexadecane*	16.5–28.0	$0.7864 \pm 0.0003$	$-6.402 \pm 0.133$	-0.999	0.7736
<i>n</i> -heptadecane†	20.0–40.0	$0.7915 \pm 0.0001$	$-6.743 \pm 0.026$	-0.999	0.7780
1-heptadecene*	10.5–28.0	$0.8015 \pm 0.0003$	$-6.431 \pm 0.139$	-0.999	0.7892

\*From White (1974).

†From American Petroleum Institute (1953).

TABLE II  
SUMMARY OF PROPERTIES OF ALIPHATIC HYDROCARBONS  
RELEVANT TO THIS STUDY\*

Hydrocarbon	Melting point	Molecular weight	$n_D$	$\epsilon = n_D^2$
	°C			
<i>n</i> -dodecane	-9.6	170.34	1.4216	2.021
<i>n</i> -tetradecane	6.0	198.40	1.4290	2.042
<i>n</i> -hexadecane	18.0	226.45	1.4345	2.056
<i>n</i> -heptadecane	22.0	240.48	1.4369	2.065
1-heptadecene	11.0	238.46	1.4432	2.083

\* As published in the *CRC Handbook of Chemistry and Physics*.  $n_D$  is the index of refraction at 20°C at the wavelength of the sodium D line.

### Calculations

The various calculations referred to in this work were performed on a Wang Laboratories (Tewksbury, Mass.) 600-6TP programmable calculator. Hard copies of programs for capacitance data reduction, calculation of interfacial tension, calculation of specific capacitance, and calculation of interfacial adsorption will be supplied upon request.

### Materials

All experiments were performed in unbuffered ( $\text{pH} \approx 6$ )  $1.00 \times 10^{-1}$  M NaCl prepared as described elsewhere (White, 1973). Glycerol monooleate (GMO) was obtained from Sigma Chemical Co. (St. Louis, Mo.). It migrated as a single spot on silica gel thin-layer plates using ether-benzene-ethanol-acetic acid (40:50:2:0.2 by volume) as a developer (Freeman and West, 1966) and on  $\text{AgNO}_3$  impregnated silica gel using chloroform-acetic acid (99.5:0.5 by volume) as a developer (Mahadevan, 1967). The glycerol monooleate was lyophilized from benzene and dispersed (20 mg/ml) in 99.5% *n*-dodecane (C12), *n*-tetradecane (C14), or *n*-hexadecane (C16) (LaChat Chemicals, Inc., Chicago Heights, Ill.) which had been passed through alumina just before use. Heptadecane dispersions of GMO (20 mg/ml) were prepared at 25°C from 99.7% *n*-heptadecane (C17) (Chemical Samples Co., Columbus, Ohio) used without further purification.

The apparatus and techniques for forming membranes have been described elsewhere (White and Thompson, 1973). Temperature was measured using a small (1 mm diam) glass encased thermistor probe attached to a DC bridge constructed in the laboratory. The probe was placed in the chamber near the aperture for the duration of an experiment. The warming or cooling rate during controlled temperature changes was about 0.1–0.3°C/min.

## RESULTS

### Specific Capacitance Measurements

The bulk lipid solutions were applied to the aperture at a temperature of 25–30°C. No measurements were made for 30–60 min after the black film was formed to assure that equilibrium was attained and that solvent disproportionation (Andrews and Haydon, 1968) was complete. Microlenses of disproportionated solvent generally appeared within 3 min after full black and became well developed and evenly distributed in about 10 min. The effects of microlenses on measurements of specific capacitance have

been discussed in detail by White and Thompson (1973). The temperature was slowly lowered after the waiting period to about 1°C and then slowly returned to the starting temperature. A complete run on a single aged membrane generally required 2–3 h. Great care was taken to insure that the films remained flat throughout the experiment since “bulges” lead to erroneous area estimates.

Data on single membranes is described below. No effort was made to average results from different experiments since the values of specific geometric capacitance rarely varied more than 1% between membranes formed from the same solvent.

The results of measurements of  $C_g$  made on a film formed from GMO dispersed in *n*-dodecane (C12) are shown in Fig. 1. The primary observation is that  $C_g$  increases as temperature decreases. The warming and cooling curves are quite similar except for a slight hysteresis. The two curves differ in that the cooling curve is more irregular than the warming curve and is shifted to the left. The irregularities may be due to fluctuations caused by mobile microlenses. The most important observation is the abrupt change in slope between 16 and 18°C. This slope change is assumed to be caused by the GMO phase transition which occurs at about 15°C (Pagano et al., 1973). The transi-

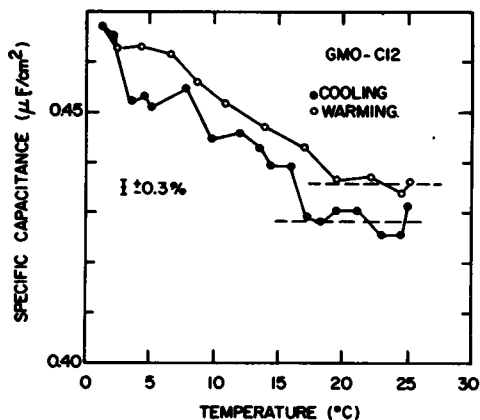


FIGURE 1

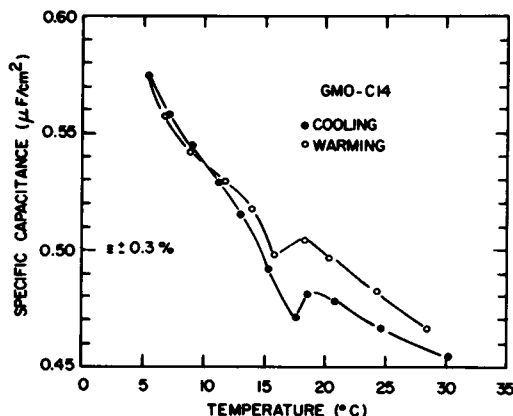


FIGURE 2

FIGURE 1 Temperature dependence of the specific geometric capacitance ( $C_g$ ) of a planar bi-layer membrane formed from glycerol monooleate (GMO) dispersed in *n*-dodecane (C12). The approximate precision ( $\pm 0.3\%$ ) of the measurements is indicated.  $C_g$  generally increases as  $T$  decreases. Note the change in slope of  $C_g(T)$  at approximately 17°C which is probably due to the GMO phase transition. There is a second faint disturbance in  $C_g(T)$  at about 5°C. The cooling (●) and warming curves (○) agree quite well but there is some hysteresis. The irregularities of the cooling curve may be due to the disproportionation of solvent into microlenses. Cooling and warming rate is about 0.3°C/min.

FIGURE 2 Temperature dependence of the specific geometric capacitance ( $C_g$ ) of a planar bi-layer membrane formed from glycerol monooleate (GMO) dispersed in *n*-tetradecane (C14). The approximate precision ( $\pm 0.3\%$ ) of the measurements is indicated.  $C_g(T)$  has abrupt changes in slope between 15 and 18°C which are probably due to a phase transition in the GMO. There are also inflections in  $C_g(T)$  between 5 and 10°C. Cooling and warming rates were about 0.1°C/min. The C14 freezes at 6°C. If temperature is lowered beyond this point the membrane ruptures.

tion temperature of C12 should occur at about  $-9.6^{\circ}\text{C}$  (Table II). The irregularities observed in the  $C_g(T)$  curves around  $5^{\circ}\text{C}$  may also be important.

Fig. 2 shows data for a film formed from GMO dispersed in *n*-tetradecane (C14). These curves also show a well-defined break in  $C_g(T)$  between  $16$  and  $18^{\circ}\text{C}$  consistent with the data on C12 films. There is also a hint of an additional inflection between  $5^{\circ}$  and  $10^{\circ}\text{C}$ . The major difference between the C12 and C14 films is that  $C_g$  is greater for C14 membranes consistent with the observations of Andrews et al. (1970). The difference can be attributed to the fraction of bilayer volume occupied by solvent. Whenever the temperature was lowered beyond the melting point of C14 ( $+6^{\circ}\text{C}$ ) the films ruptured. During the warming phase the films were most likely to rupture at  $16^{\circ}$ – $18^{\circ}\text{C}$  although this occurred infrequently.

Data obtained from a film formed using *n*-hexadecane (C16) as a solvent are shown in Fig. 3. The novel feature of this solvent system is that the annulus (Plateau-Gibbs border) of the film freezes at about  $16^{\circ}\text{C}$  without the film rupturing. This process has been described in detail elsewhere (White, 1974). Arrow *A* in Fig. 3 indicates the temperature at which the annulus of the film was observed to freeze upon cooling and arrow *D* the temperature at which the annulus melted upon warming. The melting point of C16 (Table II) occurs at about the same temperature as the phase transition of the GMO. Consequently, it is difficult to separate the effects of the two transitions as far as the capacitance measurements are concerned. White (1974) has suggested that as the hexadecane in the film freezes it disproportionates into microlenses leaving extensive regions of bilayer free of solvent. This effect leads to thinner bilayer regions and concomitantly higher capacitances but can account for only about one-half of the capacitance increase. The other half of the increase is likely due to the GMO phase transition.

There is a well-defined second inflection in the  $C_g(T)$  curve of Fig. 3 which appears at about  $10^{\circ}\text{C}$ . During cooling very bright "pin-points" appeared in the films at about the same temperature (arrow *B*) but disappeared upon warming past  $10^{\circ}\text{C}$  (arrow *C*). These bright spots appeared to be distinct from the microlenses but whether they were in fact is not known. Variations in  $C_g(T)$  at around  $10^{\circ}\text{C}$  were also observed in C12, C14, and C17 (*vide infra*) suggesting that some structural change is actually occurring at this temperature. This particular membrane ruptured at  $17^{\circ}\text{C}$  (arrow *D*) as the annulus began to melt. The relative maximum in  $C_g$  which occurred just prior to breakage may be due to unaccounted for changes in membrane area since below the freezing point of the annulus, the area was assumed to remain constant and was taken as the mean of five determinations as reported previously (White, 1974).

Comparison of the C14 data and the C16 data suggests that if the solvent freezing point is greater than the GMO transition temperature, the membrane-annulus system can be frozen without rupturing the film. Therefore, a few measurements were made on films formed from *n*-heptadecane (C17) to test this hypothesis and to separate the GMO and solvent transitions. The experiments with C14 represent the case for which the solvent transition ( $T_s$ ) occurs at a lower temperature than the GMO transition ( $T_g$ ). The experiments with C16 represent the case for which  $T_s \simeq T_g$  and the ex-

periments with C17 the  $T_s > T_g$  case. The results of two experiments with C17 are shown in Fig. 4. The arrow marks the temperature ( $\approx 21^\circ\text{C}$ ) at which the annulus froze. In general, as temperature was lowered  $C_g$  increased and reached a maximum of about  $0.685 \mu\text{F}/\text{cm}^2$  just before the freezing of the solvent. Concomitant with the solvent freezing there was an abrupt decrease in  $C_g$ . There was an abrupt increase in  $C_g$  at about  $10^\circ\text{C}$  and usually the membranes ruptured shortly after this increase occurred. In only one case was it possible to take a heptadecane membrane through a complete cooling-warming cycle. This is illustrated in Fig. 4 ( $\bullet, \circ$ ). Between  $20^\circ\text{C}$  and  $10^\circ\text{C}$   $C_g$  increases relatively slowly and two types of behavior are seen.  $C_g$  may in-

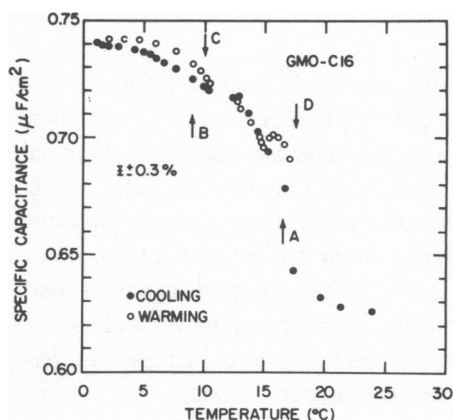


FIGURE 3

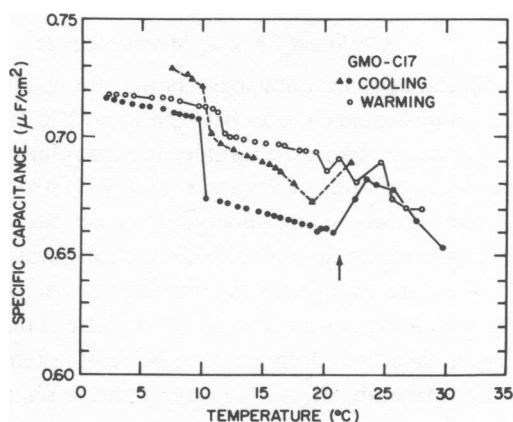


FIGURE 4

FIGURE 3 Temperature dependence of the specific geometric capacitance ( $C_g$ ) of a planar bilayer membrane formed from glycerol monooleate (GMO) dispersed in *n*-hexadecane (C16). The approximate precision ( $\pm 0.3\%$ ) of the measurements is indicated. The unique feature of system is that the annulus (Torus or Plateau-Gibbs border) freezes (arrow A) at about the melting point of the C16 ( $\sim 16^\circ\text{C}$ ) but the membrane does not rupture. The large change in  $C_g(T)$  observed between 15 and  $20^\circ\text{C}$  is probably due to a combination of solvent "freeze-out" (White, 1974) and the GMO phase transition. There is an additional change in slope in  $C_g(T)$  at about  $10^\circ\text{C}$ . Concomitant with the slope change is the appearance of bright "pin-points" in the film on cooling (arrow B) which disappear upon warming (arrow C). The annulus melted at the temperature indicated by arrow D and the film ruptured. Film rupture did not occur for most films, however. The peak seen just before rupture may be an artifact. The cooling and warming rates were about  $0.1^\circ\text{C}/\text{min}$ .

FIGURE 4 Temperature dependence of the specific geometric capacitance ( $C_g$ ) of a planar bilayer membrane formed from glycerol monooleate (GMO) and *n*-heptadecane (C17). In this system the annulus is observed to freeze at  $21^\circ\text{C}$  (arrow) which is  $5\text{--}7^\circ\text{C}$  above the expected GMO transition. Data from two membranes are shown. The data ( $\bullet, \circ$ ) represent the only experiment in which a C17 membrane could be taken through a complete cooling-warming cycle. In all other experiments the membranes ruptured between 8 and  $10^\circ\text{C}$  ( $\Delta$ ). The abrupt change in  $C_g$  at  $10^\circ\text{C}$  was always observed and coincides with the temperature at which secondary inflections were observed in  $C_g(T)$  for membranes formed from C12–C16. Just before the C17 freezing,  $C_g(T)$  passes through a maximum which corresponds to the value expected for a solvent-free fluid bilayer. Sometimes there is no evidence of the primary GMO transition ( $\bullet, \circ$ ) while at other times ( $\Delta$ )  $C_g(T)$  changes in a manner suggesting the transition is present.

crease linearly with decreasing  $T$  or it may undergo a slope change between 16 and 18°C. In any case, the thermal phase transition expected for the GMO at about 15°C is not as clearly revealed as in the C14 and C16 experiments. It is interesting that the maximum  $C_g$  ( $0.685 \mu\text{F}/\text{cm}^2$ ) obtained at  $\sim 25^\circ\text{C}$  just before the freezing of the annulus is precisely the value of  $C_g$  a fluid GMO film should have if it were absolutely free of solvent (White, 1974) suggesting that C17 is completely disproportionated from the true bilayer portion of the film. It should be noted in this regard that the value of  $C_g$  obtained at around  $5^\circ\text{C}$  is about the same as obtained from C16 films at the same temperature (see Fig. 8). The conclusion may be that solvents with chain lengths greater than or equal to 17 carbons are completely excluded from the true bilayer portions of the films at  $25^\circ\text{C}$ .

### *Interfacial Tension Measurements*

The capacitance data suggests that the GMO molecules in the bilayer films undergo organizational changes between 15 and  $20^\circ\text{C}$  and perhaps between 5 and  $10^\circ\text{C}$ . These changes are likely the result of thermal phase transitions. The calorimetric and optical reflectivity study of Pagano et al. (1973) strongly supports this contention. If the GMO molecules are in fact undergoing phase transitions, then the average area per molecule and the molecule-molecule interactions should change in the process and one should be able to see changes in the interfacial tension of the bulk lipid solutions against water. For example, in the absence of a phase transition the surface pressure of an absorbed monolayer will decrease with decreasing temperature resulting in an increase in interfacial tension. If, on the other hand, a phase transition occurs in which the average area per molecule decreases more rapidly with temperature than expected from decreases in thermal energy, the surface pressure will increase and the interfacial tension will consequently decrease. Thus, measurements of the interfacial tension of the bulk lipid against water are of considerable importance.

The interfacial tension ( $\gamma$ ) of a GMO-C14 solution against 0.1 M NaCl as a function of temperature is shown in Fig. 5.  $\gamma$  clearly decreases as temperature is decreased implying that surface pressure increases as a result of changes in the area per molecule produced by a phase transition. However, a change in the adsorption equilibrium could cause a similar result. Separate linear regression lines were fitted through the low temperature points and the high temperature points (Table III). The slopes of the two curves are statistically different. The curves intersect at  $18.7^\circ\text{C}$  which is reasonably close to the transition temperature of GMO. The points were also fitted with a second order polynomial (Table IV). The minimum in this curve occurs at  $8.6^\circ\text{C}$  which is close to the second temperature ( $5$ – $10^\circ\text{C}$ ) at which inflections in  $C_g(T)$  are seen. Whether or not these two temperatures are distinct and meaningful is not clear but they correspond closely with the changes in slope seen in the  $C_g(T)$  curves.

Fig. 6 shows the temperature dependence of the interfacial tension of a GMO-C12 solution against 0.1 M NaCl. The behavior of  $\gamma$  is qualitatively like that of the C14 solutions. The curve through the points in this case is the second order polynomial fit (Table IV) which has a minimum at  $11.2^\circ\text{C}$ . Two straight lines were also fitted to



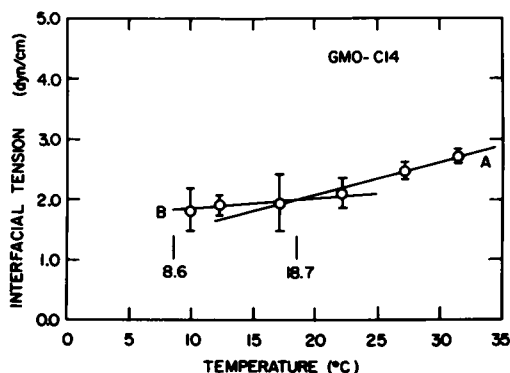


FIGURE 5

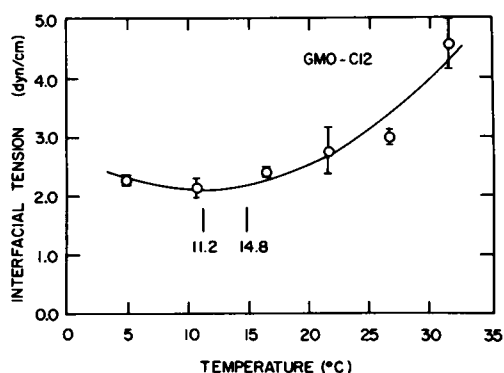


FIGURE 6

FIGURE 5 Temperature dependence of the interfacial tension ( $\gamma$ ) of a GMO-C14 dispersion against 0.1 M NaCl. The important results are (a) the general decrease in  $\gamma$  with decreasing temperature and (b) the apparent slope change at 18.7°C. The straight lines were fitted to points over two temperature ranges using the method of least squares (see Table III). The two lines intersect at 18.7°C which is close to the expected GMO primary transition temperature. The data can also be fitted with a second order polynomial with a minimum at 8.6° (Table IV) which is close to the secondary  $C_g(T)$  deviations observed between 5 and 10°C. These data support the contention that the GMO is undergoing a phase transition. The error bars indicate the standard deviations of the means of three determinations at each temperature.

FIGURE 6 Temperature dependence of the interfacial tension ( $\gamma$ ) of a GMO-C12 dispersion against 0.1 M NaCl. The behavior is similar to that seen in Fig. 5. In this case, the curve through the points is that obtained by fitting a second order polynomial (Table IV) with a minimum at 11.2°C. The data can also be fitted with two straight lines which intersect at 14.8°C (Table III). The error bars indicate the standard deviations of the means of three determinations at each temperature.

TABLE III  
INTERFACIAL TENSION OF GLYCEROL MONOOLEATE (GMO)-ALKANE DISPERSIONS  
AGAINST 0.1 M NaCl AS A FUNCTION OF TEMPERATURE

Solvent	Temperature range	$\gamma_o \pm \text{SD}$	$(d\gamma/dT) \pm \text{SD}$	Correlation coefficient	Intercept temperature
	°C	dyn/cm	$10^{-3} \text{ dyn/cm/}^\circ\text{C}$		°C
<i>n</i> -dodecane	4.9–16.5	$2.165 \pm 0.225$	$9.69 \pm 19.3$	0.449	14.8
	16.5–26.6	$1.383 \pm 0.178$	$62.6 \pm 8.1$	0.992	
<i>n</i> -tetradecane	10.0–20.0	$1.680 \pm 0.120$	$17.2 \pm 8.9$	0.887	18.7
	20.0–31.5	$0.992 \pm 0.142$	$54.1 \pm 5.6$	0.989	
<i>n</i> -hexadecane	16.5–31.5	$1.306 \pm 0.193$	$48.7 \pm 8.6$	0.930	—

The concentration of GMO in all cases was 20 mg/ml which is well above the critical micelle concentration. Interfacial tension was determined from photographs of droplets of the aqueous phase resting on a Teflon surface immersed in the lipid dispersion. The data were fitted to the equation  $\gamma = \gamma_o + (d\gamma/dT)T$  over two temperature ranges. Breaks in  $\gamma(T)$  occurred at 18.7°C and 14.8°C for tetradecane and dodecane, respectively. These temperatures correspond approximately with major inflections in the  $C_g(T)$  curves (Figs. 1 and 2).

TABLE IV  
INTERFACIAL TENSION OF GLYCEROL MONOOLEATE (GMO)-ALKANE  
DISPERSIONS AGAINST 0.1 M NaCl AS A FUNCTION OF TEMPERATURE

Solvent	$\gamma_o \pm \text{SD}$	$a \pm \text{SD}$	$b \pm \text{SD}$	Correlation coefficient	Minimum
	<i>dyn/cm</i>	<i>dyn/cm/°C</i>	$10^{-3} \text{ dyn/cm/}^\circ\text{C}^2$		$^\circ\text{C}$
<i>n</i> -dodecane	$2.798 \pm 0.443$	$-0.122 \pm 0.056$	$5.42 \pm 1.49$	0.974	11.2
<i>n</i> -tetradecane	$1.973 \pm 0.178$	$-0.0282 \pm 0.0194$	$1.65 \pm 0.46$	0.993	8.6

Data were obtained as described in Table III but in this case they were fitted to the equation  $\gamma = \gamma_o + aT + bT^2$ . The minima in the curves occur at about the same temperature at which minor inflections are observed in the  $C_g(T)$  curves.

the data (Table III) and these intersect at 14.8°C. The means of the minima and the intersections (Fig. 5 and 6) are 9.9 and 16.8°C, respectively. The interfacial tension data for GMO-C16 is shown in Fig. 7. The lipid solution froze at about 16°C precluding data collection below this temperature. However, interfacial tension decreases with decreasing temperature over the range examined. The linear regression data are shown in Table III.

The interfacial tension data taken together with the calorimetric and optical reflectivity data of Pagano et al. (1973) suggest that the observed changes in specific geometric capacitance are caused in part by GMO thermal phase transitions. The interfacial tension data and the capacitance data considered together suggests that there *might* be a second temperature dependent structural change associated with the GMO not detected by calorimetry. Some of the capacitance data from Figs. 1-4 have been consolidated in Fig. 8 to facilitate comparison. The mean values of the temperature

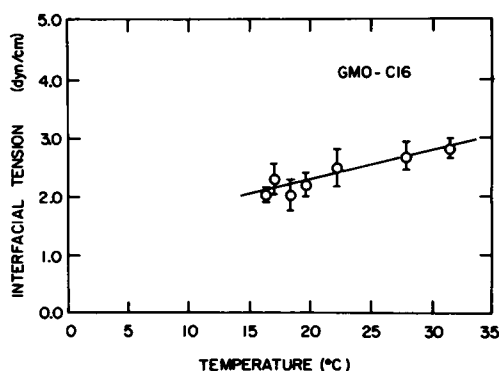


FIGURE 7 Temperature dependence of the interfacial tension ( $\gamma$ ) of GMO-16 dispersions against 0.1 M NaCl. No data were obtainable below 15°C because the dispersion freezes at this temperature. However,  $\gamma$  clearly decreases with temperature as found in Figs. 5 and 6. Such a decrease in  $\gamma$  is consistent with a phase transition. The straight line was fitted using the method of least squares (Table III). The error bars indicate the standard deviation of the mean of three measurements at each temperature.

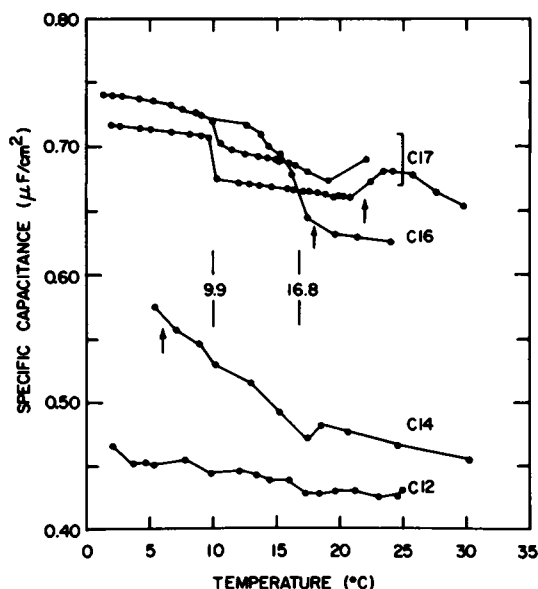


FIGURE 8 Composite of data from measurements of  $C_g(T)$  and  $\gamma(T)$ . The cooling curves of Figs. 1-4 are presented to facilitate comparison of the data. The vertical arrows indicate the temperatures at which the various solvents froze. The vertical bars at 9.9°C and 16.8°C represent the means of the two values of minima and intersections obtained in Figs. 5 and 6. Note the close correspondence between these temperatures and the slope changes in the  $C_g(T)$  curves. All of the data taken together suggest there are two temperature dependent structural changes in the bilayer. It should also be noted that  $C_g$  increases as the length of the solvent chain increases.

minima and intersections from the interfacial tension measurements (Figs. 5 and 6) are included also. The arrows indicate the melting points of the various solvents (Table II).

#### *Estimation of Glycerol Monooleate Adsorption*

It is feasible to draw conclusions about the structure of the adsorbed monolayer at the alkane-water interface from the measurements of interfacial tension. Haydon (1965) and Taylor and Haydon (1966) have suggested that uncharged molecules such as GMO should behave as a two-dimensional van der Waals gas when adsorbed at the interface. If this is true, one may write

$$(\Pi + [a_s/A^2])(A - A_o) = kT, \quad (1)$$

where  $k$  is Boltzman's constant,  $\Pi$  the surface pressure,  $A$  the area per molecule,  $A_o$  the apparent molecular cross-sectional area of the molecule, and  $a_s$  the mutual interaction energy between the various molecules. Taylor and Haydon (1966) suggest that at the oil-water interface  $a_s \simeq 0$  so that

$$\Pi = kT/(A - A_o). \quad (2)$$

This assumption is of questionable validity in the present case since thermal phase transitions probably come about via the interactions characterized by  $a_s$ . However, Eq. 2 is still useful for the purpose of estimating the interfacial adsorption. Aveyard and Briscoe (1972) have shown that Eq. 2 accurately describes the behavior of *n*-alkanols at alkane-water interfaces.

The following assumptions and procedures were adopted to calculate  $A$  and  $A_o$ . First, the number ( $N_m$ ) of GMO molecules per square centimeter of interface was estimated from the data of Andrews et al. (1970). Values of  $N_m$  at 20°C were taken as  $2.70 \times 10^{14} \text{ cm}^{-2}$  for GMO-C14 and GMO-C16 against 0.1 M NaCl and  $2.50 \times 10^{14} \text{ cm}^{-2}$  for GMO-C12 against 0.1 M NaCl. Second, the interfacial pressure was calculated from  $\Pi = \gamma_c - \gamma_m$  where  $\gamma_c$  is the interfacial tension of the clean alkane-water interface and  $\gamma_m$  is the interfacial tension of the interface with an adsorbed GMO monolayer. The data of Aveyard and Haydon (1965) were used to calculate  $\gamma_c$  at a particular temperature and  $\gamma_m$  was determined from the data of Tables III and IV. Third, above the phase transition a value of  $A_o$  (defined as  $A_o^+$ ) was established using Eq. 2 and the appropriate value of  $\Pi$  at 20°C. Values of  $A$  were then calculated as a function of temperature. Fourth, the GMO molecules were assumed to undergo a phase transition at about 16–18°C in which  $A_o$  decreased to a value of  $20 \text{ \AA}^2$  (defined as  $A_o^-$ ). Values of  $A$  were then calculated as a function of temperature below the phase transition.

The results of the calculations on interfacial adsorption for various solvent systems at two temperatures are shown in Table V.  $A_o^+$  is 29–30  $\text{\AA}^2$  which compares favorably with the mean  $A_o$  of 26  $\text{\AA}^2$  of the *n*-alkanols (Aveyard and Briscoe, 1972). At 5°C,  $A$  (not  $A_o$ ) has a value of about 27  $\text{\AA}^2$ . Measurements on CPK models of GMO indicate that the minimum area the polar group can occupy if the molecule is rotating about its long axis is about 27  $\text{\AA}^2$ . The values of  $A$  (37–40  $\text{\AA}^2$ ) above the

TABLE V  
STRUCTURE OF GMO MONOLAYERS ADSORBED AT THE  
ALKANE-0.1 M NaCl INTERFACE

	$T = 25^\circ\text{C}$		$T = 5^\circ\text{C}$	
	Calculated $A_o^+$	Assumed $A$	Assumed $A_o^-$	Calculated $A$
	$\text{\AA}^2$	$\text{\AA}^2$	$\text{\AA}^2$	$\text{\AA}^2$
<i>n</i> -hexadecane	29.17	37.28	—	—
<i>n</i> -tetradecane	29.14	37.28	20.0	27.27
<i>n</i> -dodecane	30.70	40.26	20.0	27.39

The adsorbed monolayers are assumed to obey the relation  $\Pi(A - A_o) = kT$  where  $\Pi = \gamma_c - \gamma_m$ .  $\gamma_c$  is the interfacial tension of the alkane-water interface and  $\gamma_m$  is the interfacial tension of the interface with an adsorbed GMO monolayer.  $A$  is the actual area per polar group at the interface and  $A_o$  is the minimum area per molecule attainable under conditions of infinite lateral compression.  $A_o^-$  (the low temperature  $A_o$ ) was arbitrarily taken as 20  $\text{\AA}^2$ .  $\gamma_c$  was calculated from the data of Aveyard and Haydon (1965) while  $\gamma_m$  was calculated using the data of Table III.

transition obtained from the data of Andrews et al. (1970) are greater than the values obtained by X-ray diffraction for lamellar phases of glycerol monodecanoate and glycerol monododecanoate which are 32.1 and 32.6 Å<sup>2</sup>, respectively (Reiss-Husson, 1967). The latter measurements were made on dispersions of the pure lipid in water. The presence of the solvent, differences in geometry, and the double bond in the oleate chain might be expected to cause the area per molecule to increase. Direct measurements of  $A$  by Pagano et al. (1972) for GMO-C16 films yields a value of about 40 Å<sup>2</sup>.

It should be kept in mind that the calculations outlined above are very crude and in certain respects questionable. The results, however, are not unreasonable. The essence of the calculations is to ignore molecular interactions described by  $a_s$  by setting  $a_s = 0$  in Eq. 1 and attribute the phase transition to changes in  $A_o$ . Since  $\Pi$  is being measured, it seems reasonable to suppose  $a_s$  is being accounted for implicitly. If one assumes the GMO acyl chains develop "kinks" above the phase transition because of *gauche* isomerization as proposed by Pechold (1968) and discussed by Träuble (1972), then it seems reasonable to account for the phase transition mathematically through a change in  $A_o$ .

## DISCUSSION

The data presented here indicate that planar bilayer membranes formed from glycerol monooleate (GMO) and alkane solvents undergo significant structural changes with temperature. Specific geometric capacitance ( $C_g$ ) generally increases as temperature decreases and there is a change of slope in  $C_g(T)$  at 15–18°C. The calorimetric study of Pagano et al. (1973) indicates a phase transition for GMO at about the same temperature suggesting that a phase transition also occurs in the planar bilayer membrane. The interfacial tension measurements support this hypothesis. There appears to be a second structural change at 5–10°C. This may be due to a pre-transition of the type observed about 10°C below the main transition in lecithin-water mixtures (Hinz and Sturtevant, 1972). Alternatively, and more likely, the two changes may represent the beginning and end of a single broad transition or be the result of a complex phase diagram originating from the properties of a two-component mixture. A more exact interpretation of the data between 10° and 18°C will not be possible until additional experiments are performed.

The solvent in the bilayer must have a significant effect on the detailed shape of  $C_g(T)$ . Fettiplace et al. (1971) have shown that specific capacitance depends upon solvent structure and this result is confirmed here (Fig. 8). It also seems likely that the acyl chain-solvent stoichiometry of the bilayer depends upon temperature (White, 1974). This dependence may be a result of phase separations induced by transitions of the GMO and/or the solvent. The shape of  $C_g(T)$  depends upon whether the solvent transition temperature is less than, equal to, or greater than the GMO transition temperature (Fig. 8). Finally, the presence in the film of the microlenses of solvent described by Henn and Thompson (1968) and Andrews and Haydon (1968) can also

affect measurements of specific capacitance (White and Thompson, 1973). Thus, the specific capacitance of planar bilayers will be affected by GMO and solvent phase transitions, solvent structure, acyl chain-solvent stoichiometry, and microlenses.

#### *Calculating Specific Geometric Capacitance: the Assumptions*

Insight into the structures of the planar bilayer membranes can be obtained through calculations of  $C_g$  based on various models. Eq. 3 in the Appendix shows that  $C_g$  is proportional to the ratio of the bilayer hydrocarbon dielectric coefficient ( $\epsilon_B$ ) to the bilayer hydrocarbon thickness ( $\delta_B$ ). Unless  $\epsilon_B$  or  $\delta_B$  can be independently determined, variations in  $C_g$  cannot tell us whether  $\epsilon_B$ ,  $\delta_B$ , or both are varying with temperature. Total membrane thickness and average index of refraction can be estimated using optical methods (Cherry and Chapman, 1969). Unfortunately, no such measurements are available for GMO-alkane films. X-ray diffraction studies of GMO-aqueous dispersions in a lamellar configuration could provide estimates of bilayer thickness and estimates of the area per polar group from which the dielectric coefficient could be estimated. Again, no such studies have been reported in the literature.

Lacking suitable optical or X-ray studies,  $\epsilon_B$  was estimated above the transition temperature using the equations summarized in the appendix which are based upon the assumptions of Fettiplace et al. (1971). The assumptions are that (a) the hydrocarbon interior of the film behaves as an isotropic liquid and (b) the alkane solvent and the acyl chains form ideal mixtures. Neither of these assumptions is likely to be absolutely correct. The acyl chains must be oriented to some extent causing an optical anisotropy. Lecithin-decane bilayers have an index of refraction ( $n$ ) normal to the film of 1.486 and an index parallel to the film of 1.464 (Cherry and Chapman, 1969). The respective values for  $\epsilon$  would be 2.21 and 2.14 assuming  $\epsilon = n^2$ . These numbers include, however, contributions by polar groups and, probably, contributions by microlenses. The microlenses cause serious problems since they scatter light and make the reflectance anomalously high. They probably also have an effect on birefringence because of their convex shape. It will be shown below that the microlenses probably have a negligible effect on the measurements of specific capacitance reported here. Mixtures of lipid acyl chains and alkane solvents show positive deviations from ideal behavior (Sidney Simon, personal communication). Measurements in this laboratory of the density of mixtures of alkanes with alkenes indicate the deviations are likely not to cause serious errors.

All things considered, it seems reasonable to adopt the assumptions of Fettiplace et al. (1971) until suitable optical measurements have been performed. Above the transition temperature, the acyl chains are likely to have many *gauche* isomerizations and not be fully extended which should minimize anisotropic effects. As will be shown below, the thicknesses obtained give reasonable answers. Namely, the maximum thickness obtained under any circumstances corresponds within the precision of the measurements to twice the fully extended length of the acyl chains. Pagano et al. (1973) report the average index of refraction of glyceryl monostearate-hexadecane films to be 1.427

corresponding to a dielectric coefficient of 2.04 which agrees well with the values calculated here.

Below the transition little data on the dielectric coefficient of the membrane constituents is available. In this case  $\epsilon_B$  for closest packed GMO acyl chains was calculated using Eq. 9 and 10 in the Appendix and estimates of density based on the molecular volumes published by Tardieu et al. (1973). This calculation essentially accounts for the increased polarizability per unit volume caused by the density increase.

The various equations for calculating  $C_g$  and other parameters are summarized for convenience in the Appendix. The results of the calculations based on various models are described below.

#### *Bilayer Film Structure Above the Transition*

Above the GMO phase transition the films are assumed to be in a fluid state and to be heterogeneous with solvent distributed between regions of true bilayer and regions of microlenses. The true bilayer regions will have a specific geometric capacitance  $C_g$  but the microlenses will cause the measured specific capacitance of a whole heterogeneous film to be  $C_g^A$ . The relation between the two values can usually be expressed as  $C_g^A = bC_g$  where  $b$  is a correction factor accounting for the fraction of the film area occupied by microlenses (see Appendix). Variable amounts of solvent can be trapped in films as microlenses (Pagano et al., 1972) but if the lenses have a large enough average diameter their effect on the measurements is small and  $b$  approaches unity (White and Thompson, 1973). Pagano et al. (1972) have shown the minimum amount of solvent present in GMO-hexadecane films to be  $13.7 \times 10^{-8} \text{ cm}^3$  per  $\text{cm}^2$  of film at  $25^\circ \text{C}$ . If this amount of solvent were distributed uniformly in the film, then  $C_g$  would be less than  $0.49 \text{ } \mu\text{F}/\text{cm}^2$  which is much smaller than the observed value of about  $0.625 \text{ } \mu\text{F}/\text{cm}^2$ . The conclusion must be that much of the solvent is distributed in microlenses. Larger amounts of solvent were often observed by Pagano et al. (1972). The excellent reproducibility ( $\sim 1\%$ ) of  $C_g$  suggests that the lenses must be large to minimize variations in  $C_g$  caused by variations in solvent content. Suppose the lenses were  $20 \text{ } \mu\text{m}$  in diameter and contained  $11.5 \times 10^{-8} \text{ cm}^3$  of solvent per square centimeter of film. They will have a negligible specific capacitance and occupy only 0.7% of the measured (apparent) membrane area so that  $b = 0.993$ . The volume of solvent in the true bilayer will be  $2.2 \times 10^{-8} \text{ cm}^3/\text{cm}^2$ . Assuming  $N_{AC} = 5.36 \times 10^{14} \text{ cm}^{-2}$  (from Table V), one obtains  $X_{AC} = 0.92$ ,  $F_{AC} = 0.923$ ,  $\delta_B = 29.2 \text{ } \text{\AA}$ ,  $\epsilon_B = 2.075$ ,  $C_g = 0.628 \text{ } \mu\text{F}/\text{cm}^2$ , and  $C_g^A = 0.624 \text{ } \mu\text{F}/\text{cm}^2$ . These parameters are not greatly different from those of Table VI which were calculated assuming no lenses to be present. Thus it seems reasonable to ignore the presence of the microlenses in the remainder of the discussion.

The mean specific capacitances at  $25^\circ \text{C}$  of the films of Figs. 1–4 are compared in Table VI. Also included in this table are data for GMO-decane films reported by White (1973). The composition and physical properties of each film (also shown in Table VI) were estimated using the data of Tables I, II, V, and Andrews et al. (1970)

TABLE VI  
COMPARISON OF THE COMPOSITION AND PHYSICAL PARAMETERS OF THE  
FOUR FILMS SHOWN IN FIGS. 1-4 AT 25°C

Solvent	$C_g$ $\mu F/cm^2$	$\epsilon_B$	$\delta_B$ $\text{\AA}$	$X_{AC}$	$F_{AC}$
<i>n</i> -decane	0.4057	2.036	44.4	0.458	0.567
<i>n</i> -dodecane	0.432	2.052	42.1	0.526	0.596
<i>n</i> -tetradecane	0.475	2.064	38.5	0.670	0.702
<i>n</i> -hexadecane	0.625	2.075	29.4	0.917	0.919
<i>n</i> -heptadecane	0.680	2.077	27.0	0.999	0.999

Calculations were made using the equations of White (1974) and the data of Tables I, II, and V. Data obtained for *n*-decane films (White, 1973) is also included.  $X_{AC}$  is the mole fraction of GMO acyl chains in the film,  $F_{AC}$  is the volume fraction occupied by the acyl chains,  $\epsilon_B$  is the dielectric coefficient of the film, and  $\delta_B$  the thickness.

and the equations described in the Appendix. Fig. 9 is based upon Table VI and shows the volume fraction ( $1 - F_{AC}$ ) of the bilayer occupied by solvent plotted against the molecular volume of the solvent. The amount of solvent in the true bilayer apparently depends upon the size of the solvent molecules in agreement with the findings of Andrews et al. (1970) and Fettiplace et al. (1971).

The important observation of Table VI is the dependence of bilayer thickness upon

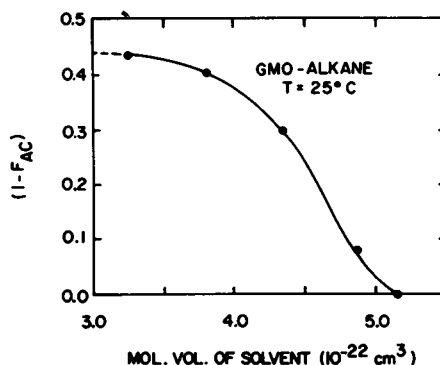


FIGURE 9 Volume fraction ( $1 - F_{AC}$ ) of bilayer membrane occupied by solvent molecules as a function of the molecular volume of the *n*-alkane solvent at 25°C. This graph is based on the data presented in Table VI. Proceeding from left to right the points represent *n*-decane, *n*-dodecane, *n*-tetradecane, *n*-hexadecane, and *n*-heptadecane. The volume fraction was calculated using the equations of White (1974) (see appendix) assuming the bilayer is in a fluid state above the phase transition and contains no microlenses. These results are consistent with those of Fettiplace et al. (1971) which show that as the length of the solvent molecule increases, the number of solvent molecules in the bilayer decreases. It appears that heptadecane and longer solvents will be totally excluded from the true bilayer regions of the film at 25°C. The longer solvents are probably excluded because they tend to occupy interfacial area but have no polar group to prevent energetically unfavorable water-hydrocarbon contacts. Short solvents can be contained near the center of the bilayer to occupy volume without necessarily occupying interfacial area.



solvent structure. The explanation of this observation is that the volume fraction ( $1 - F_{AC}$ ) of the film occupied by solvent decreases with increasing solvent chain length. ( $1 - F_{AC}$ ) decreases from about 0.43 for *n*-decane to almost zero for *n*-heptadecane. At the same time the thickness decreases from 44.4 Å (*n*-decane) to 27.0 Å (*n*-heptadecane). The fully extended length of the GMO acyl chain in the all-*trans* conformation (excluding the  $\overset{|}{\underset{|}{\text{C}}}=\text{O}$  group) can be estimated from the molecular volumes of Tardieu et al. (1973) as 22.3 Å assuming the cross-sectional area of the chain to be 20 Å<sup>2</sup>. Therefore, the hydrocarbon thickness of a bilayer with fully extended acyl chains would be 44.6 Å meaning that in *n*-decane bilayers the acyl chains spend at least part of the time in the all-*trans* conformation as suggested by Andrews et al. (1970). In the *n*-heptadecane bilayers the average acyl chain length is only about 60% of the fully extended length.

Laser Raman spectroscopy (Mendelsohn, 1972) indicates that in the liquid state *n*-hexadecane and oleic acid alkyl chains are predominantly in the form of *gauche* isomers. The *gauche* rotations about CH<sub>2</sub>—CH<sub>2</sub> bonds are likely to form “kinks” (Träuble, 1972) or the related *gauche*<sup>+</sup>–*gauche*<sup>−</sup> rotation pairs (Flory, 1969; Seiter and Chan, 1973) which effectively shorten the alkyl chain. The formation of a single “kink” (involving two *gauche* rotations) in the GMO acyl chain would shorten the chain by 1.27 Å while maintaining the long axis of the molecule perpendicular to the plane of the membrane. There are 16 bonds available in the chain for *gauche* rotations and one can estimate using the arguments of Nagle (1973) that there are likely to be about seven such rotations per chain. If these are in the form of “kinks,” the chain will be shortened relative to the all-*trans* conformation by ~4.5 Å or the bilayer thickness decreased by ~9 Å to 35.6 Å. This is ~9 Å thicker however, than estimated for the heptadecane membranes. 14 *gauche* rotations per chain would be required to reduce the bilayer thickness to 27 Å. Alternatively, the axis of the kinked chain may not be perpendicular to the plane of the bilayer. If the long axes were tilted on the average about 41° (= cos<sup>−1</sup>[27/35.6]), then the bilayer would be 27 Å thick. Statistical “bends” in the acyl chains such as proposed by McFarland and McConnell (1971) would also cause a decreased thickness. Having *gauche* rotations which did not occur in pairs to give “kinks” would lead to bent chains.

It is surprising that the *n*-decane membranes apparently achieve a thickness equal to twice the all-*trans* length considering that *gauche* isomerizations of the acyl chains are likely to be abundant above the transition temperature. The all-*trans* conformation of hexadecane and oleic acid is usually observed only in the solid state (Mendelsohn, 1972). Andrews et al. (1970) have suggested, however, that the acyl chains need be fully extended for only a small fraction of the time in order for the bilayer to have an average thickness of twice the fully extended length. They propose a gradient of *n*-decane molecules across the bilayer thickness such that the solvent is located primarily in the center of the bilayer. This suggests the following model. Imagine that at some time *t* a small patch of bilayer has all acyl chains in the contracted state and that there is sufficient solvent between the monolayers to cause the thickness to be 44.4 Å.

At some later time  $t'$  some of the acyl chains will be fully extended and the space vacated by the extension process will be filled with decane. As time progresses there could be a continual exchange between space occupied by acyl chains and space occupied by solvent molecules. This model is consistent with the  $^{13}\text{C}$  NMR study by Godici and Landsberger (1974) which suggests that the acyl chains of egg lecithin undergo a "whipping" motion causing the chains to swing up toward the glycerol skeleton. The acyl chains of GMO might be expected to have similar motions. The presence of the *n*-decane may permit such motions to become fully developed and result in transient extensions to the all-*trans* state.

It is reasonable for several reasons to assume that the solvent is concentrated near the center of the bilayer. Numerous magnetic resonance studies of phospholipid multilayers and vesicles indicate a gradient of fluidity across the bilayer with the  $-\text{CH}_2-$  groups near the glycerol skeleton being more constrained than those near the terminal  $-\text{CH}_3$  (see for example Hubbel and McConnell, 1971; Levine et al., 1972). Thus bilayers are more fluid toward the center and one would expect the solvent to fit into the structure more easily in the more fluid regions. Also, if the solvent molecules were near the surface of the bilayer they would tend to occupy the same interfacial area as the GMO but would not be shielded from the aqueous phase by a polar group. The solvent molecules can, however, occupy volume without occupying interfacial area by being located in the interior of the bilayer. This reasoning may explain the small volume fraction of the bilayer occupied by the longer chain solvents such as *n*-hexadecane and *n*-heptadecane. These molecules will tend to align parallel to the acyl chains (see discussions by Vandenheuvel [1968] and Phillips et al. [1969]) and have the same length and volume as the acyl chains. If they occupied 43% of the bilayer volume as decane does, they would necessarily occupy a large fraction of the interface without being shielded from the aqueous phase by a polar group. Therefore, it is thermodynamically unreasonable to expect large amounts of the longer chain solvents to be present in the bilayer.

#### *Bilayer Film Structure Below the Transition*

The comparison in Fig. 8 of the  $C_g(T)$  data for films formed with various solvents suggests that the structures of the films below the GMO transition temperature differ. The important observation is that the values of  $C_g$  for tetradecane (C14) and dodecane (C12) films are much smaller than for hexadecane (C16) and heptadecane (C17) films. Table VI and Fig. 9 suggest that much more solvent must remain in the true bilayer regions of the films formed with shorter alkanes. The findings of White (1974) strongly support the hypothesis that the true bilayer regions of the C16 films are largely free of solvent which means the GMO molecules must be tightly packed and generally extended below the phase transition temperature. Films formed from C17 have about the same value of  $C_g$  at  $1^\circ\text{C}$  as those formed from C16 supporting the hypothesis that there are large regions of solvent-free bilayer. The interfacial tension data of Tables III, IV, and V indicate that the GMO molecules in C12 and C14 films also undergo a phase transition implying that they necessarily become more tightly packed in some way even

though significant amounts of solvent must remain in the true bilayer. In order to change the GMO packing and still retain significant amounts of solvent, the structure of the C12 and C14 films must be somewhat different from C16 and C17 films below the phase transition. Above the phase transition all of the films probably have a similar fluid structure differing primarily in the amounts of solvent present (see discussion in previous section).

Consider first GMO-C16 films. As the GMO molecules undergo the phase transition, they must become more tightly packed and extended. This process probably leads to the exclusion of C16 from the structure into microlenses which, if large enough, have a negligible effect on  $C_g$ . The tetradecane data (in lieu of hexadecane data) of Table V suggests that below the phase transition the concentration of acyl chains increases. The dielectric coefficient  $\epsilon_B$  must consequently increase since the number of polarizable molecules per unit volume has increased.  $\epsilon_B$  can be estimated using Eq. 7 and 8 of the Appendix if the density of the film can be estimated. The density is estimated from the molecular volumes given by Tardieu et al. (1973) as  $0.883 \text{ g/cm}^3$  assuming the acyl chains are tightly packed and have a cross-sectional area of  $20 \text{ \AA}^2$ .  $\epsilon_B$  is calculated to be 2.26. It was mentioned earlier that the fully extended length of the acyl chain is about  $22.3 \text{ \AA}$  so that the thickness  $\delta_B$  of a bilayer with fully extended chains normal to the bilayer surface will be  $44.6 \text{ \AA}$ .  $C_g$  is calculated under these circumstances to be  $\sim 0.49 \text{ \mu F/cm}^2$  which is much smaller than the measured value at  $1^\circ\text{C}$  of  $0.740 \text{ \mu F/cm}^2$  (Fig. 3). The model is clearly inadequate.

Examination of Table V reveals that the area per molecule at the interface is about  $27 \text{ \AA}^2$  which is larger than the assumed value of  $20 \text{ \AA}^2$  for the tightest packing configuration of the acyl chains. X-ray diffraction studies of lecithins (Tardieu et al., 1973) indicate that  $20 \text{ \AA}^2$  is a reasonable area per acyl chain below the phase transition and it is thus reasonable to assume the GMO acyl chains are nearly in the tightest packing configuration. A reasonable way of having the acyl chains in this configuration while still having the area/molecule ratio in the interface be  $27 \text{ \AA}^2$  is for the fully extended molecules to be oriented at an angle  $\theta$  with respect to the normal of the bilayer such that the projected cross-sectional area of the acyl chain is  $27 \text{ \AA}^2$ .  $\theta$  is found from  $\cos \theta = 20/27$  to be about  $40^\circ$ . This structure for the GMO bilayer is analogous to the  $L\beta'$  prime structure for highly hydrated synthetic lecithin systems (Tardieu et al., 1973) which have the acyl chains tilted from the normal by  $30\text{--}40^\circ$ . If the GMO molecules are indeed tilted, then the thickness of the bilayer will be  $44.6 \cos \theta \approx 33 \text{ \AA}$  thicker than the value observed above the transition (Table VI). Unfortunately  $C_g$  is calculated in this case to be only  $0.61 \text{ \mu F/cm}^2$  if  $\epsilon_B$  is 2.26. A value of  $0.74 \text{ \mu F/cm}^2$  is obtained, however, if one assumes  $\epsilon_B$  equals 2.76. If one assumes  $\epsilon_B$  is 2.26, then  $\delta_B = 27 \text{ \AA}$  for  $C_g = 0.74 \text{ \mu F/cm}^2$ . This is the same thickness calculated above the transition for heptadecane films. If this is the correct thickness, then certainly the acyl chains must be packed quite differently than above the transition. There are two possibilities. The chains might be fully extended and tilted  $53^\circ$  from normal causing the ratio of area/polar group to be  $\sim 33 \text{ \AA}^2$ . Alternatively, the acyl chains could slide past one another causing the bilayer to become a symmetrical monolayer with

an area/molecule ratio of  $\sim 40 \text{ \AA}^2$  (the same as above the transition). Note that a bilayer thickness of  $27 \text{ \AA}$  is only  $4.7 \text{ \AA}$  thicker than the fully extended acyl chain length of  $22.3 \text{ \AA}$ . This latter model is remarkably similar to that proposed for potassium stearate soaps in the gel phase by Vincent and Skoulios (1966). They determined the area per polar group to be  $38.8 \text{ \AA}^2$  and the "bilayer" thickness to be  $25.2 \text{ \AA}$ . The estimated fully extended length of the molecule was estimated to be  $23.5 \text{ \AA}$ .

Below the phase transition, the structure of films formed from *n*-tetradecane and shorter solvents must be different from those formed from the longer solvents because of the large differences in the specific geometric capacitance. It is reasonable to assume the films formed with the shorter solvents retain a fair amount of solvent in the true bilayer regions and that the solvent is located near the central plane of the bilayer. The solvent could be accommodated in the center even though the GMO appears to undergo a phase transition if the acyl chains have a bent configuration as proposed by McFarland and McConnell (1971). This configuration would permit the "bent" portions of the molecules near the surface to have the all-*trans* conformation and be tightly packed. The "straight" portions of the molecules near the center could remain fluid due to the presence of the solvent. It is known that the inclusion of *n*-decane disrupts the  $L\beta'$  structure of synthetic lecithins below the phase transition (Tardieu et al., 1973). It is not unreasonable to expect the acyl chain of GMO to have contiguous lengths in the all-*trans* and *gauche* conformations. Mendelsohn (1972) has shown that the introduction of cholesterol into egg lecithin vesicles above the phase transition decreases the amount of *gauche* isomerization and increases the content of all-*trans* conformations consistent with the model of Rothman and Engelman (1972) for the cholesterol-lecithin interaction. In this model, the rigid planar portion of the cholesterol molecule constrains the acyl chains near the glycerol group to be in the all-*trans* conformation. The flexible alkyl chain of cholesterol, however, permits the terminal length of the acyl chain to remain fluid. Lippert and Peticolas (1971) have shown that the presence of cholesterol in dipalmitoyl lecithin multilayers below the phase transition causes increased fluidity probably by disrupting cooperative interactions between acyl chains. Short alkane solvents could have a similar disruptive effect in the center of the bilayer.

Suppose, then, that the  $11 \text{ \AA}$  of the GMO acyl chain near the polar group is in the all-*trans* conformation and tilted  $40^\circ$  with respect to the normal so that the area per polar group is about  $27 \text{ \AA}^2$  (Table V). Suppose that the remainder of the chain is able to undergo *gauche* isomerization and is aligned roughly parallel with the normal to the plane of the membrane. If the mole fraction on *n*-tetradecane in the fluid interior is 0.05, then the central zone will be  $19 \text{ \AA}$  thick with a dielectric coefficient of 2.1. This central fluid zone will be bounded by two gel-like zones about  $8.25 \text{ \AA}$  thick with a dielectric coefficient of 2.26. Thus, the bilayer can be represented by three capacitors in series. The  $C_g$  obtained under these circumstances is  $0.54 \text{ \mu F/cm}^2$ . This value of  $C_g$  is very close to that observed near  $10^\circ \text{ C}$  (Fig. 2) which is the temperature at which the secondary transition is observed.

Mr. Robert Anderson provided excellent technical assistance during the course of this work, and numerous discussions with Doctors Richard Pagano, Adrian Parsegian, and Sidney Simon were very helpful.

The research was supported by grants from the National Science Foundation (GB-40054) and the National Institute of Neurological Diseases and Stroke (NS-10837). The Guggenheim Multiple Sclerosis Foundation provided a generous grant at a crucial stage of the investigations.

Received for publication 17 July 1974.

## APPENDIX

The specific geometric capacitance of a planar bilayer membrane is given by

$$C_g = \epsilon_0 \epsilon_B / \delta_B, \quad (3)$$

where  $\epsilon_0 = 8.854 \times 10^{-14}$  F/cm,  $\epsilon_B$  is the dielectric coefficient of the hydrocarbon core, and  $\delta_B$  the thickness. The thickness can be estimated from  $C_g$  only if  $\epsilon_B$  is known or can be estimated.

Above the phase transition the bilayer is assumed to be in a fluid state and the acyl chains and solvent molecules assumed to form ideal mixtures (Fettiplace et al., 1971). White (1974) has derived equations for calculating  $\epsilon_B$  and  $\delta_B$  under these circumstances which account for the temperature dependent changes of density and dielectric coefficient of the acyl and solvent chains. These equations are summarized as follows:

$$\epsilon_B = F_{AC} \epsilon_{AC} + (1 - F_{AC}) \epsilon_S, \quad (4)$$

where  $F_{AC}$  is the volume fraction of the film occupied by surfactant acyl chains,  $\epsilon_{AC}$  the dielectric coefficient of the acyl chains, and  $\epsilon_S$  the dielectric coefficient of the solvent.

$$\delta_B = \frac{N_{AC}}{N_A} \left[ \left( \frac{1}{X_{AC}} - 1 \right) \frac{M_S}{\rho_S} + \frac{M_{AC}}{\rho_{AC}} \right], \quad (5)$$

where

$$X_{AC} = N_{AC} / (N_{AC} + N_S). \quad (6)$$

$N_{AC}$  is the number of acyl chains per unit area of film,  $M$  the molecular weight,  $\rho$  the absolute density (grams per cubic centimeter), and  $N_A$  Avogadro's number. The subscripts  $AC$  and  $S$  refer to the acyl chains and solvent, respectively. The volume fraction ( $F_{AC}$ ) of the bilayer occupied by acyl chains is given by

$$F_{AC} = [1 + ([1/X_{AC}] - 1)(M_S \rho_{AC} / M_{AC} \rho_S)]. \quad (7)$$

The density of most aliphatic hydrocarbons depends linearly upon temperature and consequently

$$\rho_i(T) = g_i + h_i T, \quad (8)$$

where  $g_i$  and  $h_i$  are constants and  $i$  represents either  $AC$  or  $S$ . The dielectric coefficient of the solvent and acyl chains can be calculated from

$$\epsilon_i(T) = \frac{1 + 2(\rho_i^2 m + \rho_i b_i)/M_i}{1 - (\rho_i^2 m + \rho_i b_i)/M_i}, \quad (9)$$

where

$$b_i = \frac{\epsilon_i(20) - 1}{\epsilon_i(20) + 2} \cdot \frac{M_i}{\rho_i(20)} - m\rho_i(20), \quad (10)$$

with  $m$  being about  $-3 \text{ cm}^6/\text{g} \cdot \text{mol}$ .

The above equations assume that no microlenses of the type described by Andrews and Haydon (1968) are present. The effect of the microlenses on measurements of  $C_g$  can be estimated using the following equation derived by White and Thompson (1973):

$$C_g^A = C_g(1 - [2V_{SL}/\theta a]) + (2\epsilon_o\epsilon_S V_{SL}/\theta a[\delta_B + \theta a/2]), \quad (11)$$

where  $V_{SL}$  is the volume of solvent trapped in the microlenses,  $a$  is the average radius of the microlenses, and  $\theta$  is taken as  $2^\circ$  (Haydon and Taylor, 1968). In many cases the term on the right is negligible and one may write

$$C_g^A = bC_g, \quad (12)$$

where  $C_g^A$  is the apparent (i.e. measured) specific geometric capacitance and  $b = (1 - 2V_{SL}/\theta a)$ .

## REFERENCES

- AMERICAN PETROLEUM INSTITUTE. 1953. Selected Values of Physical and Thermodynamic Properties of Hydrocarbons and Related Compounds, A.P.I. Project 44. Carnegie Press, Washington, D.C.
- ANDREWS, D. M., and D. A. HAYDON. 1968. *J. Mol. Biol.* **32**:149.
- ANDREWS, D. M., E. D. MANEV, and D. A. HAYDON. 1970. *Spec. Discuss. Faraday Soc. No. 1*. 46.
- AVEYARD, R., and B. J. BRISCOE. 1972. *J. Chem. Soc. Faraday Trans. II*. **68**:478.
- AVEYARD, R. and D. A. HAYDON. 1965. *Trans. Faraday Soc.* **61**:2255.
- BRANTON, D. 1966. *Proc. Natl. Acad. Sci. U.S.A.* **55**:1048.
- C.R.C. Handbook of Chemistry and Physics. 1965. The Chemical Rubber Company, Cleveland, Ohio. 46th edition.
- CHAPMAN, D., R. M. WILLIAMS, and D. B. LADBROOKE. 1967. *Chem. Phys. Lipids*. **1**:445.
- CHERRY, R. J., and D. CHAPMAN. 1969. *J. Mol. Biol.* **40**:19.
- ELETR, S., D. ZAKIM, and D. A. VESSEY. 1973. *J. Mol. Biol.* **78**:351.
- ENGLEMAN, D. M. 1971. *J. Mol. Biol.* **58**:153.
- FETTIPLACE, R., D. M. ANDREWS, and D. A. HAYDON. 1971. *J. Membr. Biol.* **5**:277.
- FLORY, P. J. 1969. *Statistical Mechanics of Chain Molecules*. Interscience, Inc. N.Y.
- FREEMAN, C. P., and D. WEST. 1966. *J. Lipid Res.* **7**:324.
- GODICI, P. E., and F. R. LANDSBERGER. 1974. *Biochemistry*. **13**:362.
- HANAI, T., D. A. HAYDON, and J. TAYLOR. 1964. *Proc. R. Soc. Lond.* **281A**:377.
- HAYDON, D. A. 1965. *Annu. Rep. Chem. Soc.* **62**:9.
- HAYDON, D. A., and J. TAYLOR. 1968. *Nature (Lond.)* **217**:239.
- HENN, F. A., and T. E. THOMPSON. 1968. *J. Mol. Biol.* **31**:227.
- HINZ, H.-J., and J. M. STURTEVANT. 1972. *J. Biol. Chem.* **247**:6071.
- HUBBELL, W. L. and H. M. MCCONNELL. 1969. *Proc. Natl. Acad. Sci. U.S.A.* **64**:20.
- HUBBEL, W. L., and H. M. MCCONNELL. 1971. *J. Am. Chem. Soc.* **93**:314.
- KRASNE, S., G. EISENMAN, and G. SZABO. 1971. *Science (Wash. D.C.)*. **174**:412.
- LADBROOKE, B. D. and D. CHAPMAN. 1969. *Chem. Phys. Lipids*. **3**:304.
- LEVINE, Y. K., N. J. M. BIRDSALL, A. G. LEE, and J. C. METCALFE. 1972. *Biochemistry*. **11**:1416.

- LIPKIN, M. R., J. A. DAVISON, W. T. HARVEY, and S. S. KURTZ. 1944. *Ind. Eng. Chem.* **16**:55.
- LIPPERT, J. L. and W. L. PETICOLAS. 1971. *Proc. Natl. Acad. Sci. U.S.A.* **68**:1572.
- MAHADEVAN, V. 1967. *Lipid Chromatographic Analysis*, Vol. 1. G. V. Marinetti, editor. Marcel Dekker, Inc., New York. 191.
- McFARLAND, B. G., and H. M. McCONNELL. 1971. *Proc. Natl. Acad. Sci. U.S.A.* **68**:1274.
- MELCHIOR, D. L., and H. J. MOROWITZ. 1972. *Biochemistry*. **11**:4558.
- MENDELSON, R. 1972. *Biochim. Biophys. Acta*. **290**:15.
- MUELLER, P., D. O. RUDIN, H. T. TIEN, and W. C. WESCOTT. 1962. *Circulation*. **26**:1167.
- OVERATH, P., F. F. HILL, and I. LAMNEK-HIRSCH. 1971. *Nat. New Biol.* **234**:264.
- NAGLE, J. F. 1973. *J. Chem. Phys.* **58**:252.
- PAGANO, R. E., R. J. CHERRY, and D. CHAPMAN. 1973. *Science (Wash. D.C.)*. **181**:557.
- PAGANO, R. E., J. M. RUYSSCHAERT, and I. R. MILLER. 1972. *J. Membr. Biol.* **10**:11.
- PECHOLD, W. 1968. *Kolloid-Z. Z. Polym.* **228**:1.
- PHILLIPS, M. C., R. M. WILLIAMS, and D. CHAPMAN. 1969. *Chem. Phys. Lipids*. **3**:234.
- REISS-HUSSON, F. 1967. *J. Mol. Biol.* **25**:363.
- ROTHMAN, J. E., and D. M. ENGELMAN. 1972. *Nat. New Biol.* **237**:42.
- SEITER, C. H. A., and S. I. CHAN. 1973. *J. Am. Chem. Soc.* **95**:7541.
- STAICOPOULUS, D. N. 1962. *J. Colloid Sci.* **17**:439.
- STARK, G., R. BENZ, G. W. POHL, and J. JANKO. 1972. *Biochim. Biophys. Acta*. **266**:603.
- STEIM, J. M., M. E. TOURTELLOTTE, J. C. REINERT, R. N. McELHANEY, and R. L. RADER. 1969. *Proc. Natl. Acad. Sci. U.S.A.* **63**:104.
- TARDIEU, A., V. LUZZATI, and F. C. REMAN. 1973. *J. Mol. Biol.* **75**:711.
- TAYLOR, J., and D. A. HAYDON. 1966. *Discuss. Faraday Soc. No. 42*. 51.
- TRÄUBLE, H. 1972. *Biomembranes* Vol. 3. F. Kreuzer and J. F. G. Slegers, editors. Plenum Publishing Co., New York, 197.
- VANDENHEUVEL, F. A. 1968. *Chem. Phys. Lipids*. **2**:372.
- VINCENT, J. M., and A. SKOULIOS. 1966. *Acta Crystallogr.* **20**:432.
- WHITE, S. H. 1970 a. *Biophys J.* **10**:1127.
- WHITE, S. H. 1970 b. *Biochim. Biophys. Acta*. **196**:354.
- WHITE, S. H. 1973. *Biochim. Biophys. Acta*. **323**:343.
- WHITE, S. H. 1974. *Biochim. Biophys. Acta*. **356**:8.
- WHITE, S. H., and T. E. THOMPSON. 1973. *Biochim. Biophys. Acta*. **323**:7.
- WILKINS, M. H. F., A. E. BLAUROCK, and D. M. ENGELMAN. 1971. *Nat. New Biol.* **230**:72.